

## Predictive model based on artificial neural network for estimating the adsorption of nickel and lead on a natural and synthetic support

Hézia Bouarar<sup>a</sup>, Mounir Bouhedda<sup>b,\*</sup>, Hakima Cherifi<sup>a</sup>

<sup>a</sup>Laboratory of Biomaterials and Transport Phenomena (LBMPT), University of Medea, Nouveau Pôle Urbain, Medea 26000, Algeria, emails: bouarar.hizia@univ-medea.dz (H. Bouarar), ha\_cherifi@yahoo.fr (H. Cherifi)

<sup>b</sup>Laboratory of Advanced Electronic Systems (LSEA), University of Medea, Nouveau Pôle Urbain, Medea 26000, Algeria, email: bouhedda.m@gmail.com

Received 20 June 2023; Accepted 5 December 2023

---

### ABSTRACT

In this study, the adsorption process of nickel and lead on natural supports, specifically bentonite and activated carbon, was modeled using an artificial neural network (ANN). The primary objective was to quantify the adsorption yield of the adsorbed metal. The developed ANN model was validated to assess its effectiveness in predicting experimental data sets. For both nickel and lead, the mean square error of the model was calculated to be  $3.72 \times 10^{-4}$ , indicating a highly accurate model. In addition, the trained ANN was used to predict the influence of several parameters, including pH, contact time, initial metal concentration, temperature, material, and adsorbent concentration, on the adsorption of these metals using the two different adsorbents. The ANN was well constructed and optimized using a 6-10-1 topology. The performance of the model was evaluated using test data, which showed high correlation coefficients for ( $R^2$ ) values of 0.99430 and 0.99439 for the validation and test data, respectively. These results indicate the robustness and accuracy of the ANN model in predicting the adsorption behavior of nickel and lead on bentonite and activated carbon.

*Keywords:* Adsorption; Activated carbon; Artificial neural network; Bentonite; Lead; Modeling; Nickel; Prediction

---

### 1. Introduction

The contamination of water by organic and inorganic substances is a significant environmental issue [1,2]. Mineral pollutants, such as heavy metals, are of particular environmental concern due to their high density, which exceeds  $5 \text{ g/cm}^3$  [3,4]. These pollutants are typically found in trace amounts in the environment and consist of a range of substances, such as arsenic, zinc, manganese, nickel, cobalt, lead, cadmium, mercury, and copper. The distinct chemical properties of heavy metals enable their toxicity to humans as well as flora and fauna [5]. Lead is notably recognized as a hazardous micropollutant among these metals, and its toxicity remains significant even in trace concentrations [6–8]. In contrast, nickel and its inorganic compounds are

generally considered less toxic. Based on the International Agency for Research on Cancer's categorization, nickel compounds fall under the group 1 category as carcinogens for humans while metallic nickel is classified under group 2B as a possible human carcinogen [9,10].

Several methods exist to eliminate heavy metals, including adsorption, which is a cost-effective approach known for its efficacy in retaining and eliminating inorganic and organic compounds [11,12]. Currently, multiple authors in [13,14] have recognized activated carbon as a versatile adsorbent, supported by multiple studies demonstrating its effectiveness. Other viable options for adsorbent materials include activated alumina, goethite, kaolin, hydroxides [15,16], and clays like bentonites [17–22].

---

\* Corresponding author.

Previous studies have demonstrated that nonlinear models effectively characterize the complexity of adsorption phenomena. Two approaches must be undertaken by researchers to develop these models. The first approach requires mathematical modeling, incorporating a deep understanding of chemistry, biology, and other sciences to describe a highly complex equation, specifically in the context of this paper. The second approach utilizes experimental data to elucidate the relationship between input parameters and resulting outputs [23]. This method is applied in processes characterized by complex physical experimentation or substantial nonlinear behavior, utilizing a multivariate parameter database. This approach directly pertains to the subject matter addressed herein.

The intricate and protracted process of constructing mathematical models for complex systems has motivated researchers to investigate artificial intelligence techniques as an alternative modeling approach. Artificial neural network (ANN) has become a valuable modeling tool in recent years for studying various wastewater treatment methods [24–26]. ANNs can learn patterns and relationships from data, enabling approximation of the behavior of underlying systems. ANNs are a powerful and promising modeling tool in various fields due to their ability to capture nonlinear relationships, handle high-dimensional data, and adapt to noisy or incomplete information [27].

ANNs offer significant advantages as they provide a learning mechanism for developing intelligent models to predict adsorption yield. ANNs can effectively learn from input-output data to identify complex patterns and relationships within the adsorption process. Through the acquisition of relevant data, ANNs can accurately predict the amount of adsorption. Recent studies have utilized ANNs to examine the adsorption of Ni and Pb onto various sorbents. Specifically, [24,25,28] have implemented ANN modeling to investigate fluoride adsorption systems.

This work aims to maximize gains and advantages by targeting two distinct objectives. The first objective revolves around environmental considerations, specifically, the elimination of two toxic heavy metals with demonstrated harmful effects. In addressing this issue, the study explores natural materials, carbon and bentonite, as potential solutions for mitigating the environmental impact of toxic waste. The second objective of this study is to optimize and predict adsorption yield using intelligent models to facilitate decision-making and improve industrial operations.

To meet these objectives, a singular ANN is synthesized using the MATLAB Neural Networks toolbox (version 2018a). The ANN is trained with a database gathered from available literature sources [8,29] and through experimental measures. This enables the ANN to learn and predict the adsorption yield (%) of the two metal adsorbents. This approach not only establishes a comprehensive learning database for the ANN but also guarantees the production of dependable predictions to support the objectives of the research.

## 2. Materials and methods

We have established and optimized operating conditions based on a review of relevant literature and preliminary

experiments [30–33]. These conditions are described in detail in the following sections.

### 2.1. Data collection, pretreatment and analysis

Two metals, nickel nitrate ( $\text{Ni}(\text{NO}_3)_2$ ) and lead nitrate ( $\text{Pb}(\text{NO}_3)_2$ ), were utilized in this study. We prepared stock solutions of nickel and lead with a 1,000 mg/L concentration and kept them away from light. We then diluted the solutions in various proportions to obtain lower concentrations.

### 2.2. Adsorbates

#### 2.2.1. Bentonite

Bentonite is a white pigment powder derived from natural bentonite sourced from Maghnia (Tlemcen City, Algeria). It is obtained by grinding, sieving up to 100  $\mu\text{m}$ , and then drying the natural bentonite.

#### 2.2.2. Activated carbon

The powdered active carbon utilized in this study is LABKEM CHAR-PWA-500 by Labbox (France), with a pH of 7.50 and an ash content of 0.19%.

### 2.3. Determination of $\text{Ni}^{2+}$ and $\text{Pb}^{2+}$

To determine the levels of  $\text{Ni}^{2+}$  and  $\text{Pb}^{2+}$  in the water samples, a UV-Visible Spectrophotometer of the Shimadzu-1240 type (Japan) was employed, with measurements taken at wavelengths of  $\lambda = 240$  and 520 nm, respectively.

### 2.4. Description of the adsorption tests

The batch adsorption of nickel and lead was conducted discontinuously on a shaker by contacting a synthetic solution of nickel and lead, containing various concentrations, with a constant mass of the adsorbent. Subsequently, solid and liquid separation was accomplished by using a membrane with 0.45  $\mu\text{m}$  porosity through vacuum filtration of the sample. Moreover, we determined the concentration of each filtered sample. Finally, Eq. (1) was used to calculate the adsorption yield ( $Y(\%)$ ).

$$Y(\%) = \frac{C_{\text{in}} - C_t}{C_{\text{in}}} \times 100 \quad (1)$$

where  $C_t$ : concentration of the solution at time “ $t$ ” (mg/L);  $C_{\text{in}}$ : initial concentration (mg/L).

Various tests were conducted to study the impact of certain factors on the removal of nickel using bentonite and lead using activated carbon. These factors include the contact time, ranging from 3 to 300 min, the initial concentration of  $\text{Ni}^{2+}$  and  $\text{Pb}^{2+}$ , varying between 20 and 250 mg/L, the adsorbent dosage, ranging from 0.1 to 5 g/L, the temperature, ranging from 15°C to 60°C, and the pH of the treatment, which was between 1 and 9. The impact of pH was examined by buffering the synthetic solution of nickel and lead with HCl (0.1 N) and NaOH (0.1 N) solutions throughout the adsorption test.

2.5. Data collection

A database of adsorption performance data for two specific metals on two different adsorbents was compiled by gathering experimental data from existing literature sources [8,29] and by performing new experimental measurements under a range of initial conditions.

3. Neural modeling

3.1. Description

A multilayer ANN, often referred to as a neural network with multiple layers, is a computational model inspired by the structure and functioning of the human brain [34]. It is designed for a wide range of machine learning and pattern recognition tasks. Here is a detailed description of a multilayer ANN.

3.1.1. Input layer

The first layer of the network is called the input layer. It consists of neurons, each representing a feature or input variable. Neurons in this layer simply pass on the input values to the next layer without any processing. Each neuron corresponds to one feature in the input data [35,36].

3.1.2. Hidden layers

Between the input and output layers, there can be one or more hidden layers. These layers are where the network performs most of its computation. Neurons in each hidden layer process the information from the previous layer and pass it on to the next layer. These neurons apply weighted sums and activation functions to transform the data.

3.1.3. Weights and connections

Each connection between neurons (synapse) has an associated weight. These weights are learned during the training process. Weights determine the strength of the connection and play a crucial role in shaping the network's ability to model complex relationships within the data [37].

3.1.4. Output layer

The final layer of the network is called the output layer. Its number of neurons depends on the nature of the task. For binary classification, it might have one neuron, while for multi-class classification or regression tasks, it may have multiple neurons. The neurons in the output layer produce the network's final predictions based on the computations performed in the hidden layers [38].

3.1.5. Activation functions

Each neuron in the hidden layers and output layer typically applies an activation function to the weighted sum of its inputs. Commonly used activation function is usually the distorted hyperbolic tangent given by Eq. (2), representing the hyperbolic function. This formula calculates the output  $z$  for each neuron in the network [39].

$$z = \tanh(as) = \frac{e^{as} - e^{-as}}{e^{as} + e^{-as}} \tag{2}$$

where  $a$  is the coefficient that determines the slope of the sigmoidal function in Eq. (3) based on the expression of  $s$ .

$$s = \sum_i w_{ij}x_{ij} + b_i \tag{3}$$

where  $x_{ij}$  is the input of the  $i$ th neuron provided by the  $j$ th neuron of the previous layer;  $w_{ij}$  denotes the connection weight of connection with the  $j$ th neuron of the previous layer;  $b_i$  corresponds to the  $i$ th neuron bias.

3.2. ANN training

Multilayer ANNs are trained using a supervised learning algorithm called backpropagation. Backpropagation works by adjusting the weights of the ANN based on the error between its predictions and the known target values (Fig. 1). This process is repeated until the ANN is able to accurately predict the target values for all of the data samples in the training set.

Learning is essential for the development of ANNs, as it allows them to adapt their behavior to achieve desired results. To learn, ANNs are exposed to a set of data samples that represent the desired behavior (samples) [40]. By studying these examples, the ANN can gradually fine-tune its internal parameters (weights) to learn and replicate the samples [38]. This process results in improved overall performance and more accurate predictions.

Learning algorithms, such as the Levenberg–Marquardt algorithm, are used to update the weights of the ANN in a way that minimizes the mean square error (MSE) [39,41]. The MSE is a measure of the difference between the predicted and actual values of the target variables [42].

3.2.1. Levenberg–Marquardt algorithm

During the learning phase, various algorithms can be utilized, including the Levenberg–Marquardt algorithm. This algorithm adapts the values of the weights and through an iterative process, minimizing the errors of the output neurons (supervised learning) using Eqs. (4) and (5).

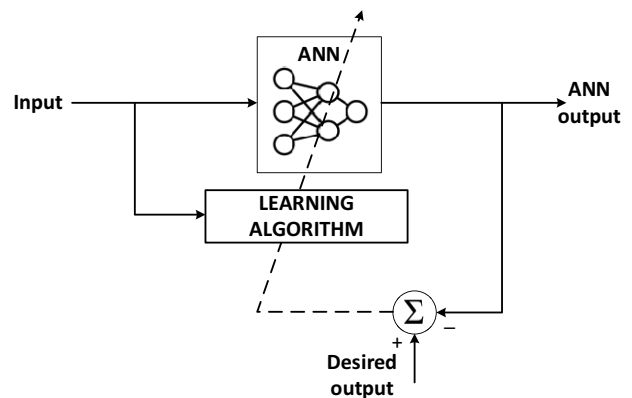


Fig. 1. Artificial neural network supervised learning.

$$w_{ij}(k) = w_{ij}(k-1) - [J^T J + \mu I]^{-1} J^T \varepsilon_i(k-1) \tag{4}$$

$$b_i(k) = b_i(k-1) - [J^T J + \mu I]^{-1} J^T \varepsilon_i(k-1) \tag{5}$$

where  $J$  is the Jacobian matrix containing the initial derivatives of errors of the neural network, while considering the weights and biases.  $K$  represents the current iteration of the learning algorithm.  $\varepsilon_i$  is the output error of the  $i$ th neuron, and  $\mu$  denotes the learning rate.

The ANN’s learning progress is governed by an index, commonly known as the mean square error (MSE). The MSE is an objective measure of the average difference, squared, between the ANNs predicted output and the actual output. It serves as a criterion for evaluating the network performance during its learning process. At times, the specific expression for the MSE can be represented by a mathematical relation, such as Eq. (6) [43]. This equation denotes a formal representation of the MSE formula used in the context of the ANN learning process.

$$MSE = \frac{1}{M} \sum_{k=1}^M \sum_{i=1}^L (y_i^k - z_i^k)^2 \tag{6}$$

where  $M$ : Levenberg–Marquardt algorithm iterations number,  $L$  is the dimension of the output layer,  $y_i$  is the  $i$ th desired output of the ANN and  $k$  denotes the current iteration.

### 3.2.2. ANN synthesis procedure

The classical development cycle of a neural network can be divided into ten steps, as shown in the flowchart in Fig. 2. These steps are preceded by four operations to construct and use a reliable representative database.

- Database collection,
- Selection of inputs and outputs of the neural model,
- Database preparation,

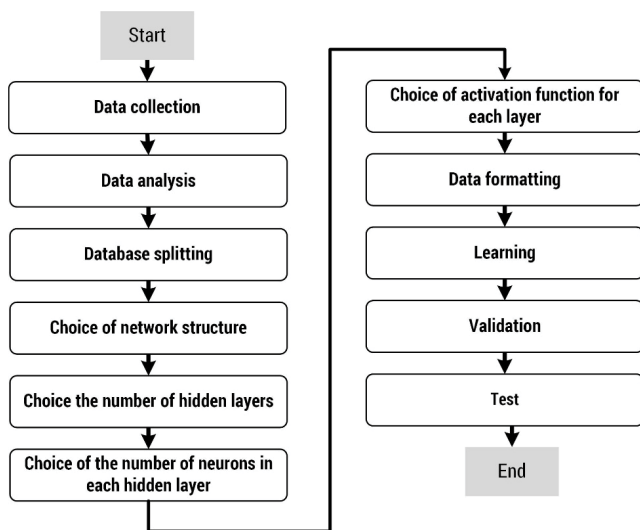


Fig. 2. Flowchart of artificial neural network design.

- Data formatting.

The following three phases are very crucial and are followed in order to synthesize a reliable ANN.

- During the initial learning phase, the ANN is trained to produce desired outputs in response to specific input, which is known as learning data. The ANN’s performance is then assessed by calculating appropriate performance indices using reference data, or test data. Even though the test data differs from the training data, it is carefully selected to align with the training data, thus ensuring consistency and evaluating the quality of ANN’s learning.
- The ANN undergoes a validation phase to assess its generalization capability, wherein additional independent data called validation data is used. This data is distinct from the training and testing data utilized in the earlier phases. By evaluating the ANN’s performance using the validation data, the model’s ability to accurately predict outputs for unseen inputs is tested and validated. This is a crucial step to ensure the ANN can accurately apply its learned patterns and relationships to new and unfamiliar data, verifying its reliability and robustness beyond the data exclusively utilized in the training and testing phases.
- Testing phase: The ANN has the capability to generate desired outputs for any given input. During the testing phase, the ANN can produce desired outputs for any given input as it has learned and generalized patterns and relationships from the training and validation phases. This ability enables the ANN to generate accurate and reliable outputs for a wide range of inputs, including those it has not previously encountered. The production phase indicates the effective implementation of the trained ANN model, enabling its use in real-world applications to generate desired outputs based on diverse inputs.

During each phase, a certain amount of data is extracted from the learning dataset which contains 1,000 samples, 500 samples for each metal. Typically, 80% of the data is reserved for the learning phase, 10% for the validation phase, and the remaining 10% for testing the ANN. Additionally, specific data preprocessing operations must be carried out to guarantee optimal outcomes during the learning phase like checking and cleaning.

### 3.2.3. Partial normalization of the database

Scaling is frequently a necessary aspect of data preparation, particularly for input data, as bounded sigmoid transfer functions are commonly utilized in static models. In this study, a distinct sub-database was utilized for the adsorbent/metal pairs. Numeric values were normalized to enhance optimization for achieving output values within the range of  $[-0.9, 0.9]$ .

### 3.3. ANN architecture

In this study, ANN model is utilized with multiple inputs, including pH, temperature, initial metal concentration,

contact time, adsorbent concentration, and matter. The ANN's output was the adsorption yield. The ANN architecture used in this study had a topology of [6-10-1], as shown in Fig. 3. Table 1 outlines the learning outcomes.

The dataset necessary for training the ANN was derived from conducted adsorption experiments. The Levenberg–Marquardt algorithm was utilized for network training.

The ANN modeling was implemented via the neural network toolbox of MATLAB (2018a). It is worth noting that a larger dataset for model training, testing, and validation would enhance the performance of the ANN architecture.

Fig. 4 illustrates the progression of the mean square error. The desired outcome is obtained after  $2 \times 10^4$  iterations. The obtained MSE for the two metals is  $3.72 \times 10^{-4}$ .

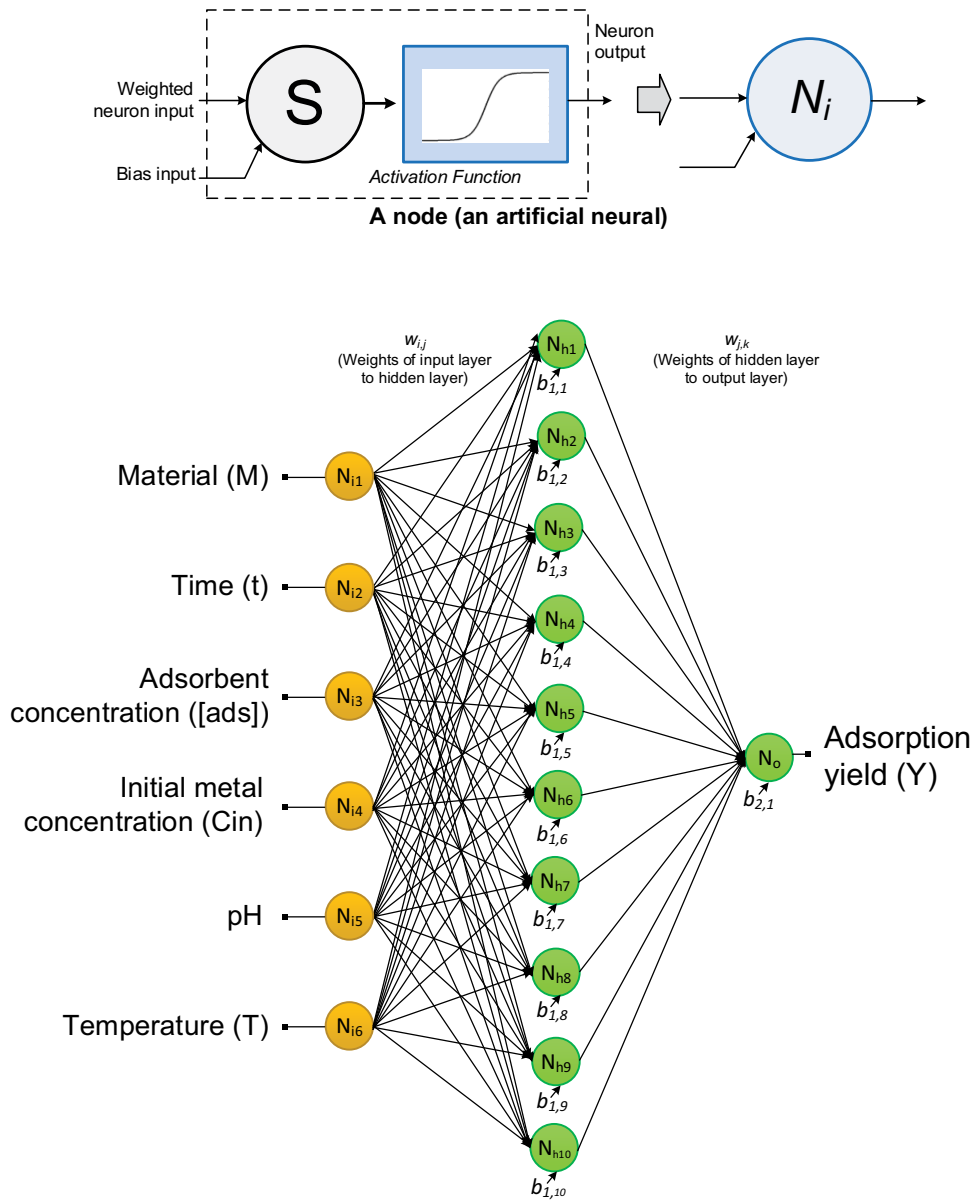


Fig. 3. Topology of adopted neural architecture.

Table 1  
Learning results

ANN description	Material	Inputs	Output	Number of hidden layers	Number of neurons in the hidden layer	Maximum epochs	MSE
1: Ni		$t$ , material, [ads],	Adsorption yield (%)	01	10	$2 \times 10^4$	$3.72 \times 10^{-4}$
2: Pb		$C_{in}$ , pH, $T$					

#### 4. Results and discussion

The synthesized ANN has demonstrated significant effectiveness in predicting the adsorption yield within the

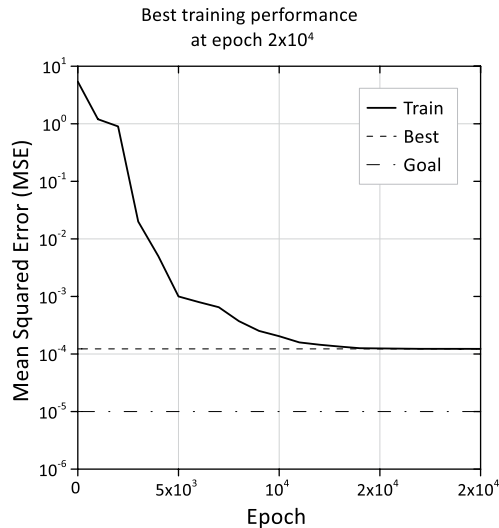


Fig. 4. Evolution of the mean square error during the artificial neural network training phase.

range of data included in the training set. The ANN's predicted efficiency for adsorption yield is comparable to the results obtained from the training and test data provided by the same network. In Table 2 comparison results are presented between predicted and experimental adsorbed yields of two metals using two types of adsorbents.

Fig. 5 illustrates the performance results of the ANN model by presenting the correlation between observed and predicted heavy metal adsorption yields. These values serve as a strong endorsement of the model's accuracy. It is evident, from the same figure, that all data points align precisely along the diagonal, and the correlation coefficients ( $R^2$ ) for both the test and validation datasets are impressively high, measuring 0.99430 and 0.99439, respectively.

Table 3 compares the training performance of synthesized ANN with other ANN models used in different studies on the adsorption of Ni(II) and/or Pb(II) using different adsorbents. The comparison results affirm that the developed ANN architecture for our prediction model is a good choice. This architecture exhibits precision, demonstrating its ability to make accurate predictions with a high level of confidence.

##### 4.1. Predicting of the adsorption of Ni on bentonite and Pb on activated carbon using ANN

The developed ANN model was used to investigate the effects of operating conditions on adsorption in nickel/

Table 2  
Comparison of the predicted and experimental adsorbed yields of the two metals by two types of adsorbents

Material 1: Ni, 2: Pb	$t$ (min)	[ads] (g/L)	$C_{in}$ (mg/L)	pH	$T$ (°C)	$Y_{exp}$ (%)	$Y_{pre}$ (%)	Absolute error
2	60	3	20	4	22	99.08	99.84	0.76
1	120	3	100	5.5	15	70.62	70.37	0.25
2	180	0.6	100	5.64	18	90.03	89.43	0.60
1	5	5	100	7.66	16	85.50	84.80	0.70
2	5	0.5	10	6	25	78.00	78.74	0.74
2	60	0.5	40	6	25	52.36	52.98	0.62
2	180	1	50	2	25	34.21	34.83	0.62
2	60	1	20	4	47	90.50	91.07	0.57
1	3	5	30	7.66	16	92.33	92.66	0.33
1	120	3	80	5	15	85.87	85.69	0.18
2	180	0.7	500	6	30	89.09	89.27	0.18
1	120	3	80	5.5	15	85.83	85.60	0.23
2	180	0.7	100	5.64	20	82.28	82.37	0.09
1	120	4	80	5.5	15	88.35	88.38	0.03
2	180	0.7	200	6	30	94.77	95.51	0.74
2	140	0.5	70	6	25	62.08	62.49	0.41
2	180	0.7	100	5.64	30	90.63	90.17	0.46
2	180	0.7	300	6	30	96.65	96.41	0.24
1	180	5	100	7.66	60	97.50	97.97	0.47
1	3	5	70	7.66	16	91.21	91.09	0.12
2	180	0.2	100	5.64	18	87.70	87.06	0.64
1	3	5	60	7.66	45	93.16	92.82	0.34
1	3	5	40	7.66	16	91.87	92.25	0.38
1	120	3	80	6	15	89.21	89.17	0.04

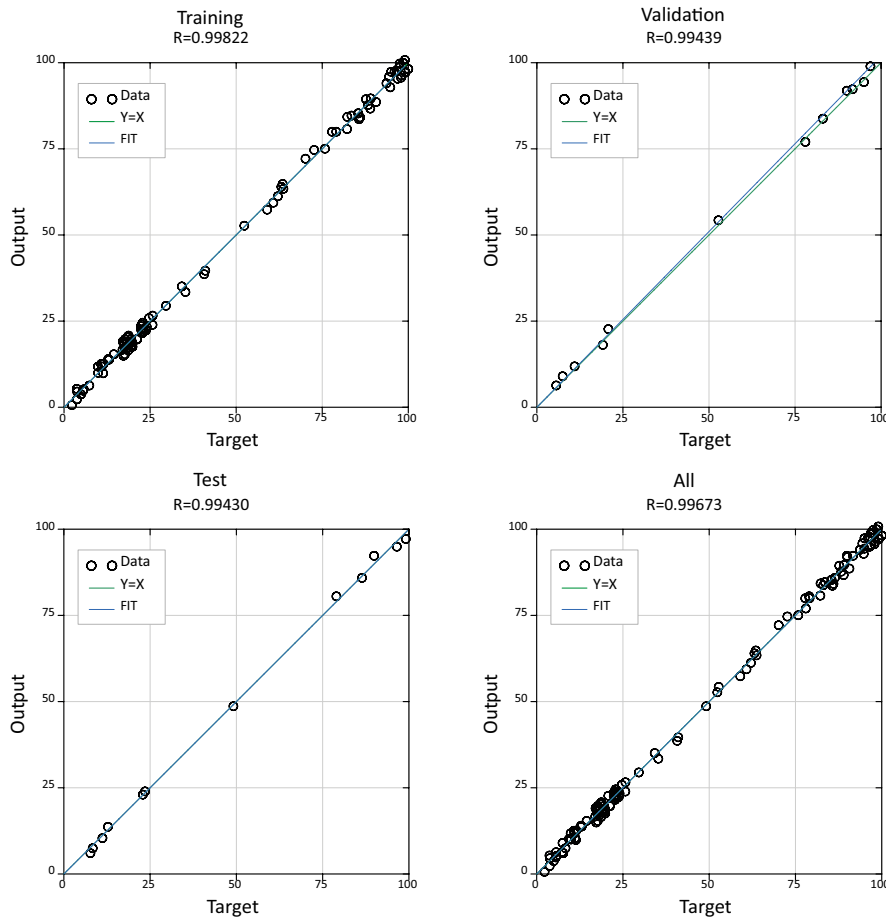


Fig. 5. Optimal neural network performance for training, testing, validation data and all data.

Table 3  
Comparison of the performance and application of this work to other works using artificial neural network prediction

References	Adsorbent	Adsorbate	R <sup>2</sup>
[44]	Ni(II)	Ultrasonically modified chitin (UM-chitin)	0.9995
[45]	Pb(II) and Ni(II)	Biochar derived from date seeds	0.9923
[46]	Pb(II)	Walnut shells functionalized with carboxylate groups	0.9915
Our work	Pb(II) and Ni(II)	Bentonite and activated carbon	0.9943

bentonite and lead/activated carbon systems. The adsorption capacities predicted by the ANN model were compared against experimental adsorption data, as shown in Figs. 6–10.

4.1.1. Effect of contact time

Fig. 6a and b display the adsorption yield plotted against contact time for nickel on bentonite and lead on activated carbon, respectively. The predicted and experimental values were obtained under different conditions, as shown in these figures. The equilibrium time was determined from Fig. 6.

The graphs indicate that both metals reach equilibrium quickly. At the start of the adsorbate–adsorbent

contact, there are numerous free sites which results in a rapid adsorption process, causing the curves to be steep initially. The binding process of heavy metals, however, decelerates gradually as the adsorption sites become occupied [47,48]. The widely reported literature indicates a two-stage adsorption mechanism, with the initial stage being fast and quantitatively dominant, while the following stage is slower and quantitatively negligible [49].

Fig. 6a shows that after 20 min of contact the nickel removal rate is close to 80%, the nickel adsorption after 120 min of treatment reaches 86.1%. Fig. 6b depicts effective lead adsorption within the initial 20-min interval, followed by stabilization leading to equilibrium. This phenomenon is explicable via molecular diffusion’s role in transporting ions to the adsorption site, until adsorption equilibrium is



reached. The behavior of all adsorption sites towards the lead ions subsequently becomes alike.

4.1.2. Effect of pH

The adsorption of metal ions is strongly influenced by the pH of the solution. Objective evaluation of these mechanisms is essential. Mechanisms that are highly dependent on pH, including ion exchange, complexation, and retention by electrostatic forces [50,51], contribute to this phenomenon.

Fig. 7a displays the adsorption yield of nickel on bentonite at various pH levels. The results indicate a positive correlation between the pH levels and adsorption efficiency. At pH = 3, the adsorption is somewhat low, whereas nearly complete removal of nickel ions (92.2%) can be achieved at pH = 7. In contrast, the pH significantly affects the removal of lead ions on activated carbon (Fig. 7b). The experimental study demonstrates that the removal efficiency varies between pH = 2 and pH = 7. The findings indicate that the retention capacity is affected by the parameter value, with pH = 6 identified as the optimal pH for achieving the highest lead ion adsorption results.

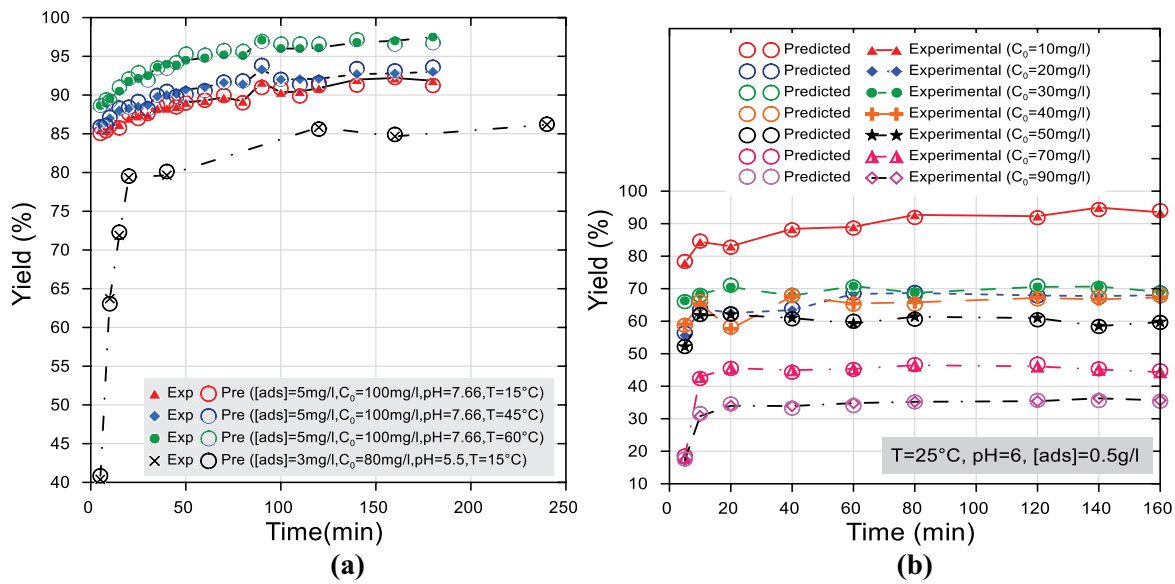


Fig. 6. Kinetics adsorption of nickel on bentonite (a) and lead on activated carbon (b) and comparison between experimental data and artificial neural network predictions.

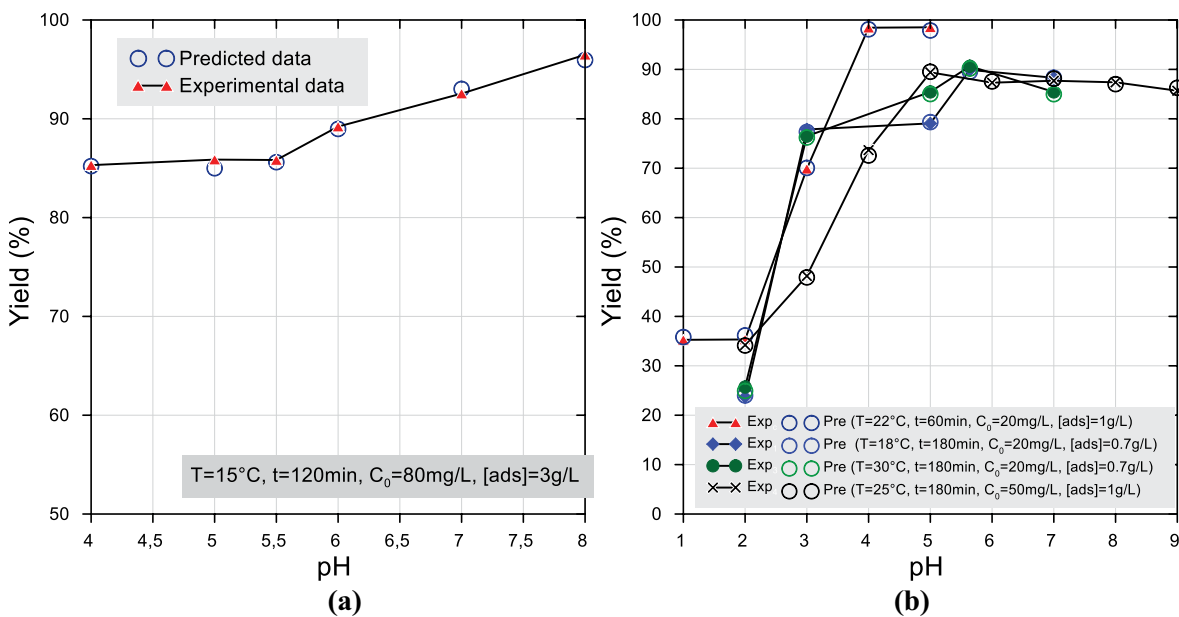


Fig. 7. Effect of pH on the adsorption of nickel on bentonite (a) and lead on activated carbon (b) and comparison between experimental data and that predicted by artificial neural network.



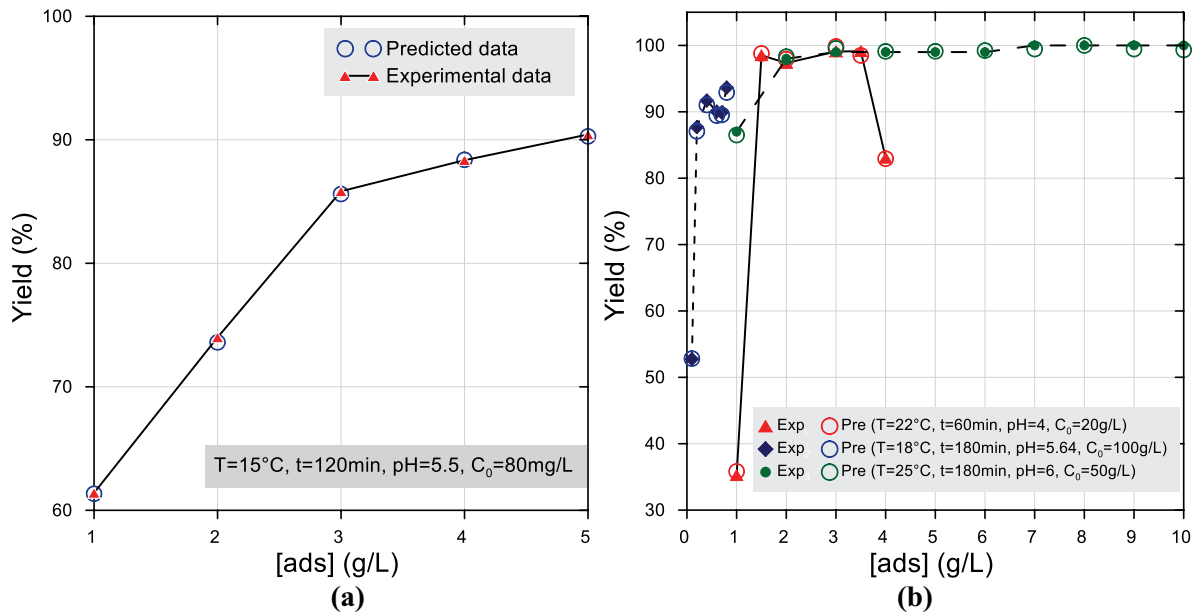


Fig. 8. Effect of initial adsorbent concentration on adsorption of nickel/bentonite (a) and lead/activated carbon (b) and comparison between experimental data and that predicted by artificial neural network.

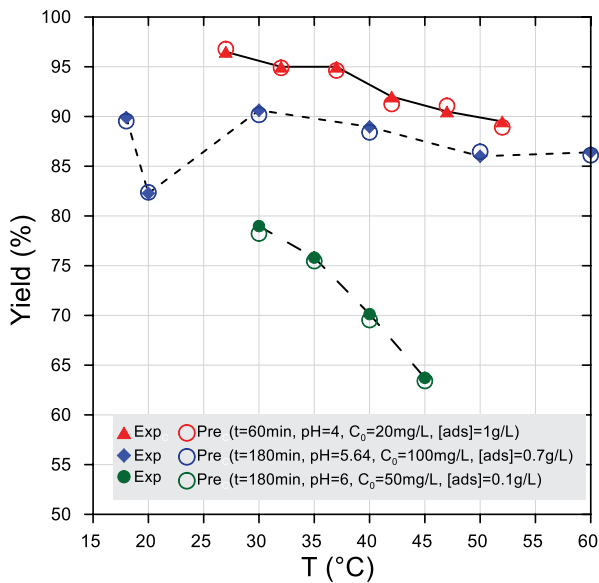


Fig. 9. Effect of temperature on the adsorption of lead on activated carbon and comparison between experimental data and artificial neural network predictions.

#### 4.1.3. Effect of the initial concentration of the adsorbent

The study investigated the impact of adsorbent concentration on the adsorption yield of Ni and Pb on bentonite and activated carbon, respectively. The findings are displayed in Fig. 8a and b.

Fig. 8a demonstrates that the rate of nickel removal by bentonite rises with the quantity of adsorbent used. This is due to the increased number of retention sites on the surface of the adsorbent when more bentonite is used. This outcome is consistent with the research of Karapinar and

Donat [52] who used bentonite as an adsorbent [52]. Based on these findings, we selected a 3 g/L quantity of bentonite as the optimal amount. Fig. 8b demonstrates that the metal removal rate increases as the quantity of adsorbent increases. Regardless of the weight of activated carbon, it effectively adsorbs more Pb<sup>2+</sup> ions. An ideal amount of 1 g of this carbon is adequate for adsorbing the maximum amount of Pb<sup>2+</sup> metal ions.

#### 4.1.4. Effect of temperature

Fig. 9 illustrates that raising the temperature up to 30°C leads to improved adsorption and an adsorption rate of 90.61%. This indicates that the temperature boosts the kinetic energy of lead ions and their diffusion towards sorption sites. However, further increased temperature reduces adsorption, suggesting exothermic adsorption of Pb<sup>2+</sup> ions. This phenomenon, known as desorption, occurs when molecules adsorbed on a surface become detached, especially due to the increase in temperature. Bias and subjective evaluations have been excluded, and the language used is clear and precise without the use of ornamental language. The sentence structure and grammar are also correct.

#### 4.1.5. Effect of the initial metal concentration

The efficacy of two adsorbents in removing nickel and lead from aqueous solutions was examined by altering the metal concentration within the 10–800 mg/L range, as shown in Fig. 10a and b.

According to Fig. 10a, the clay’s adsorption efficiency increases with an increase in initial metal concentration up to 80 mg/L. Thereafter, the adsorption efficiency of the clay continues to increase with an increase in initial metal concentration, and beyond 80 mg/L, a stabilization of the adsorbed yield is observed. Thereafter, the adsorption

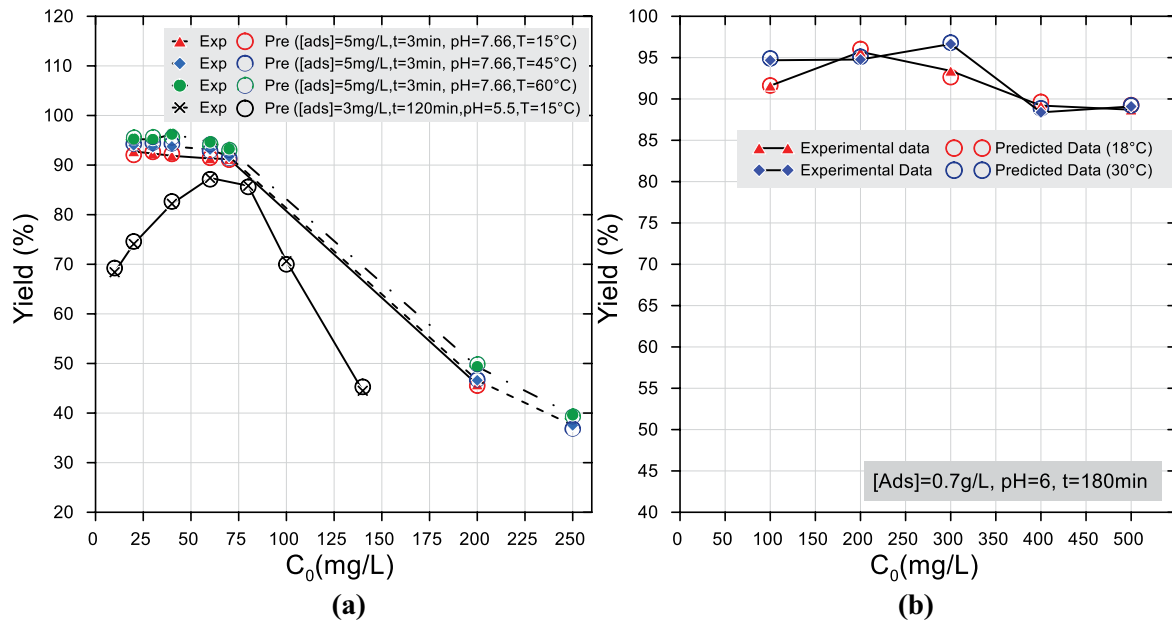


Fig. 10. Effect of initial metal concentration on nickel/bentonite (a) and lead/activated carbon (b) adsorption and comparison of experimental data with artificial neural network predictions.

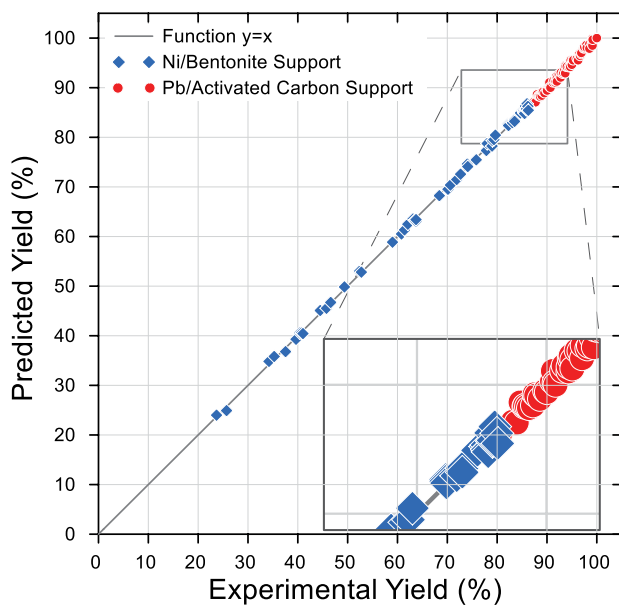


Fig. 11. Prediction of nickel and lead adsorption on bentonite and activated carbon by artificial neural network using experimental data as a parameter.

efficiency of the clay continues to increase with an increase in initial metal concentration, and beyond 80 mg/L, a stabilization of the adsorbed yield is observed. The high mobility of nickel ions in diluted solutions results in increased interaction with the adsorbent, explaining the observed phenomenon.

The impact of initial adsorbate concentrations on lead adsorption was investigated within the 100–500 mg/L range; results are presented in Fig. 10b. It was discovered

that as the initial concentration of the adsorbate increases, the adsorption efficiency decreases, and the highest removal rate of lead achieved was 95.7% at 200 mg/L.

The effectiveness of the proposed model in predicting the adsorption yields of nickel and lead on bentonite and activated carbon was demonstrated by the results obtained using artificial intelligence techniques. The predicted values were found to be in close agreement with the experimental results for both systems and under different conditions.

#### 4.2. Validation

To ensure the reliability of the constructed ANN model, we plotted the predicted values of the adsorption efficiency against the experimental data, considering all operating parameters. The grouping of points around the bisector illustrates the similarities between the experimental values, which are influenced by several parameters such as contact time, pH, temperatures, initial metal concentration and initial adsorbent concentration, and the corresponding predictions generated by the ANN model.

#### 5. Conclusion

ANNs can effectively model the complex process of adsorption. This study successfully applied an ANN model to predict adsorption of nickel and lead on natural (bentonite) and synthetic (activated carbon) supports. The optimal ANN architecture had 6 input neurons, 10 hidden neurons, and 1 output neuron. The ANN model yielded highly accurate predictions, with strong correlation between experimental and predicted adsorption results. Using 10 hidden neurons produced the highest  $R^2$  values and lowest mean squared error. The optimized and trained

ANN accurately represented both the test and validation data, with  $R^2$  values of 0.99430 and 0.99439. This demonstrates the capability of ANNs to accurately supplement traditional and complex models for predicting bioprocess parameters like adsorption.

Additionally, ANNs can effectively supplement traditional and complex models in predicting bioprocess parameters.

### Compliance with ethical standards

Conflicts of interest: The authors declare that they have no conflict of interest.

### Acknowledgment

This work is supported by the Directorate General for Scientific Research and Technological Development (DGRSDT) of the Algerian Ministry of Higher Education and Scientific Research (MESRS).

### References

- [1] WHO, World Health Report 2013: The Quest for Universal Health Coverage, World Health Organization, Geneva, Switzerland, 2013.
- [2] UNPD, Human Development Report 2009 Overcoming Barriers: Human Mobility and Development, United Nations Development Programme, New York, USA, 2009.
- [3] S. Mukherjee, Mineral Chemistry, in: Applied Mineralogy, Springer International Publishing, Dordrecht, Netherlands, 2011, pp. 54–79.
- [4] W. Kaim, B. Schwederski, A. Klein, Bioinorganic Chemistry--Inorganic Elements in the Chemistry of Life: An Introduction and Guide, John Wiley & Sons, New York, USA, 2013.
- [5] M. Larakeb, L. Youcef, S. Achour, Removal of zinc from water by adsorption on bentonite and kaolin, Athens J. Sci., 4 (2017) 47–58.
- [6] M.I. Carretero, Clay minerals and their beneficial effects upon human health. A review, Appl. Clay Sci., 21 (2002) 155–163.
- [7] R. Zhang, L. Zhou, F. Zhang, Y. Ding, J. Gao, J. Chen, H. Yan, W. Shao, Heavy metal pollution and assessment in the tidal flat sediments of Haizhou Bay, China, Mar. Pollut. Bull., 74 (2013) 403–412.
- [8] G. Mimanne, K. Benhabib, A. Bengahem, S. Taleb, Study of the adsorption of heavy metals (Pb and Cd) in aqueous solution on activated carbon and sodium montmorillonite from Western Algeria, J. Mater. Environ. Sci., 5 (2014) 1298–1307.
- [9] World Health Organization, International Agency for Research on Cancer (IARC), World Cancer Report: Cancer Research for Cancer Prevention, IARC, Geneva, Switzerland, 2020.
- [10] A.V. Ramanakumar, M.-É. Parent, B. Latreille, J. Siemiatycki, Risk of lung cancer following exposure to carbon black, titanium dioxide and talc: results from two case-control studies in Montreal, Int. J. Cancer, 122 (2008) 183–189.
- [11] S. Degremont, Memento technique de l'eau, Degremont, 2005.
- [12] M. Larakeb, L. Youcef, S. Achour, Etude comparative de l'élimination du zinc par adsorption sur la goéthite et sur la bentonite de Maghnia, LARHYSS J., 19 (2014) 87–100.
- [13] A. Politano, G. Chiarello, G. Benedek, E.V. Chulkov, P.M. Echenique, Vibrational spectroscopy and theory of alkali metal adsorption and co-adsorption on single-crystal surfaces, Surf. Sci. Rep., 68 (2013) 305–389.
- [14] C. Vagner, Caractérisation de surface d'adsorbants carbonés et étude des équilibres et cinétiques d'adsorption en phase gazeuse, Université Paul Verlaine-Metz, France, 2003.
- [15] M.D.A. Bolland, A.M. Posner, J.P. Quirk, Zinc adsorption by goethite in the absence and presence of phosphate, Aust. J. Soil Res., 15 (1977) 279–286.
- [16] M. Bali, H. Tlili, Removal of heavy metals from wastewater using infiltration-percolation process and adsorption on activated carbon, Int. J. Environ. Sci. Technol., 16 (2019) 249–258.
- [17] M. Bashir, C. Mohan, S. Tyagi, A. Annachhatre, Copper removal from aqueous solution using chemical precipitation and adsorption by Himalayan Pine Forest Residue as Biochar, Water Sci. Technol., 86 (2022) 530–554.
- [18] M. Djab, B. Makhoukhi, Adsorption of cadmium onto modified bentonites from aqueous solutions, J. Mater. Environ. Sci., 9 (2018) 2238–2246.
- [19] T. Kanti Sen, C. Khoo, Adsorption characteristics of zinc ( $Zn^{2+}$ ) from aqueous solution by natural bentonite and kaolin clay minerals: a comparative study, Comput. Water Energy Environ. Eng., 2 (2013) 1–6.
- [20] F. Mohammed-Azizi, S. Dib, M. Boufatit, Removal of heavy metals from aqueous solutions by Algerian bentonite, Desal. Water Treat., 51 (2013) 4447–4458.
- [21] F. Al Mardini, B. Legube, Effect of the adsorbate (Bromacil) equilibrium concentration in water on its adsorption on powdered activated carbon. Part 3: competition with natural organic matter, J. Hazard. Mater., 182 (2010) 10–17.
- [22] K. Addouch, S. Seddari, H. Cherifi, R. Yous, R. Khalladi, Raw clay for ibuprofen and chlortetracycline removal from aqueous solution, Desal. Water Treat., 265 (2022) 134–145.
- [23] S. Guergazi, D. Amieur, S. Achour, Elimination des Substances Humiques de deux Eaux de Surface Algériennes par Adsorption sur Charbon Actif et sur Bentonite, LARHYSS J., 13 (2013) 125–137.
- [24] S.K. Bhagat, T.M. Tung, Z.M. Yaseen, Development of artificial intelligence for modeling wastewater heavy metal removal: state of the art, application assessment and possible future research, J. Cleaner Prod., 250 (2020) 119473, doi: 10.1016/j.jclepro.2019.119473.
- [25] G. Alam, I. Ihsanullah, Mu. Naushad, M. Sillanpää, Applications of artificial intelligence in water treatment for optimization and automation of adsorption processes: recent advances and prospects, Chem. Eng. J., 427 (2022) 130011, doi: 10.1016/j.cej.2021.130011.
- [26] Z.U. Ahmad, L. Yao, Q. Lian, F. Islam, M.E. Zappi, D.D. Gang, The use of artificial neural network (ANN) for modeling adsorption of sunset yellow onto neodymium modified ordered mesoporous carbon, Chemosphere, 256 (2020) 127081, doi: 10.1016/j.chemosphere.2020.127081.
- [27] A. Kiraz, O. Canpolat, E.F. Erkan, Özer, Artificial neural networks modeling for the prediction of Pb(II) adsorption, Int. J. Environ. Sci. Technol., 16 (2019) 5079–5086.
- [28] S. Joshi, S. Bajpai, S. Jana, Application of ANN and RSM on fluoride removal using chemically activated *D. sissoo* sawdust, Environ. Sci. Pollut. Res., 27 (2020) 17717–17729.
- [29] M. Ferhat, Co-adsorption des métaux lourds sur la bentonite modifiée en présence de flocculants minéral et biologique, University of Tizi Ouzou, Algeria, 2012.
- [30] B. Anna, M. Kleopas, S. Constantine, F. Anestis, B. Maria, Adsorption of Cd(II), Cu(II), Ni(II) and Pb(II) onto natural bentonite: study in mono-and multi-metal systems, Environ. Earth Sci., 73 (2015) 5435–5444.
- [31] M.A. Rauf, M.J. Iqbal, M. Ikram, N. Rauf, Adsorption studies of Ni(II) from aqueous solution onto bentonite, J. Trace Microprobe Tech., 21 (2003) 337–342.
- [32] K. Kadirvelu, C. Faur-Brasquet, P. Le Cloirec, Removal of Cu(II), Pb(II), and Ni(II) by adsorption onto activated carbon cloths, Langmuir, 16 (2000) 8404–8409.
- [33] Y.B. Onundi, A.A. Mamun, M.F. Al Khatib, Y.M. Ahmed, Adsorption of copper, nickel and lead ions from synthetic semiconductor industrial wastewater by palm shell activated carbon, Int. J. Environ. Sci. Technol., 7 (2010) 751–758.
- [34] M. Fan, J. Hu, R. Cao, K. Xiong, X. Wei, Modeling and prediction of copper removal from aqueous solutions by nZVI/rGO magnetic nanocomposites using ANN-GA and ANN-PSO, Sci. Rep., 7 (2017) 18040, doi: 10.1038/s41598-017-18223-y.
- [35] S. Mandal, S.S. Mahapatra, M.K. Sahu, R.K. Patel, Artificial neural network modelling of As(III) removal from water by novel hybrid material, Process Saf. Environ. Prot., 93 (2015) 249–264.

- [36] R.R. Karri, J.N. Sahu, Modeling and optimization by particle swarm embedded neural network for adsorption of zinc(II) by palm kernel shell based activated carbon from aqueous environment, *J. Environ. Manage.*, 206 (2018) 178–191.
- [37] M. Bouhedda, *Architectures neuronales pour la conversion analogique/numérique*, Editions Universitaires Européennes, 2011.
- [38] S. Rebouh, M. Bouhedda, S. Hanini, A. Djellal, Neural Modeling Adsorption of Copper, Chromium, Nickel, and Lead from Aqueous Solution by Natural Wastes BT - Progress in Clean Energy, I. Dincer, C.O. Colpan, O. Kizilkan, M.A. Ezan, Eds., Volume 1: Analysis and Modeling, Springer International Publishing, Cham, 2015, pp. 341–356.
- [39] G.V.S.R. Pavan Kumar, K.A. Malla, B. Yerra, K. Srinivasa Rao, Removal of Cu(II) using three low-cost adsorbents and prediction of adsorption using artificial neural networks, *Appl. Water Sci.*, 9 (2019) 44, doi: 10.1007/s13201-019-0924-x.
- [40] J.A. Darsey, *Neural Networks in Chemical and Physical Systems*, World Scientific Press, London, UK, 2004.
- [41] S. Mirjalili, *Evolutionary Algorithms and Neural Networks*, in: *Studies in Computational Intelligence*, Springer International Publishing, Cham, Switzerland, 2019.
- [42] S. Rebouh, Utilisation des différentes techniques d'intelligence artificielle pour la modélisation du procédé de séparation par adsorption solide-liquide: étude comparative, University of Medea, Algeria, 2015.
- [43] M. Hassoun, *Fundamentals of Artificial Neural Networks*, MIT Press, Cambridge, Massachusetts, USA, 2003.
- [44] P.S. Pauletto, G.L. Dotto, N.P.G. Salau, Optimal artificial neural network design for simultaneous modeling of multicomponent adsorption, *J. Mol. Liq.*, 320 (2020) 114418, doi: 10.1016/j.molliq.2020.114418.
- [45] A. El Hanandeh, Z. Mahdi, M.S. Imtiaz, Modelling of the adsorption of Pb, Cu and Ni ions from single and multi-component aqueous solutions by date seed derived biochar: comparison of six machine learning approaches, *Environ. Res.*, 192 (2021) 110338, doi: 10.1016/j.envres.2020.110338.
- [46] M. Ashrafi, H. Borzuie, G. Bagherian, M.A. Chamjangali, H. Nikoofard, Artificial neural network and multiple linear regression for modeling sorption of Pb<sup>2+</sup> ions from aqueous solutions onto modified walnut shell, *Sep. Sci. Technol.*, 55 (2020) 222–233.
- [47] M.K. Sahu, S. Mandal, S.S. Dash, P. Badhai, R.K. Patel, Removal of Pb(II) from aqueous solution by acid activated red mud, *J. Environ. Chem. Eng.*, 1 (2013) 1315–1324.
- [48] R. Yous, R. Khalladi, H. Cherifi, Simultaneous sorption of heavy metals on Algerian bentonite: mechanism study, *Water Sci. Technol.*, 84 (2021) 3676–3688.
- [49] K. Bellir, M.B. Lehocine, A.H. Meniai, Zinc removal from aqueous solutions by adsorption onto bentonite, *Desal. Water Treat.*, 51 (2013) 5035–5048.
- [50] O. Abollino, M. Aceto, M. Malandrino, C. Sarzanini, E. Mentasti, Adsorption of heavy metals on Na-montmorillonite. Effect of pH and organic substances, *Water Res.*, 37 (2003) 1619–1627.
- [51] R. Yous, H. Cherifi, R. Khalladi, Kinetic models of competitive adsorption of cadmium-iron mixture on montmorillonite, *Desal. Water Treat.*, 221 (2021) 207–217.
- [52] N. Karapinar, R. Donat, Adsorption behaviour of Cu<sup>2+</sup> and Cd<sup>2+</sup> onto natural bentonite, *Desalination*, 249 (2009) 123–129.